Properties of alkali-metal atoms and alkaline-earth-metal ions for an accurate estimate of their long-range interactions

Jasmeet Kaur,[1] D. K. Nandy,[2,3] Bindiya Arora,[1,*] and B. K. Sahoo[2,3,†]

[1]*Department of Physics, Guru Nanak Dev University, Amritsar, Punjab 143005, India*
[2]*Theoretical Physics Division, Physical Research Laboratory, Navrangpura, Ahmedabad 380009, India*
[3]*Indian Institute of Technology Gandhinagar, Ahmedabad 382424, India*

Accurate knowledge of interaction potentials among the alkali-metal atoms and alkaline-earth ions is very useful in the studies of cold atom physics. Here we carry out theoretical studies of the long-range interactions among the Li, Na, K, and Rb alkali-metal atoms with the Ca^+, Ba^+, Sr^+, and Ra^+ alkaline-earth ions systematically, which are largely motivated by their importance in a number of applications. These interactions are expressed as a power series in the inverse of the internuclear separation R. Both the dispersion and induction components of these interactions are determined accurately from the algebraic coefficients corresponding to each power combination in the series. Ultimately, these coefficients are expressed in terms of the electric multipole polarizabilities of the above-mentioned systems, which are calculated using the matrix elements obtained from a relativistic coupled-cluster method and core contributions to these quantities from the random-phase approximation. We also compare our estimated polarizabilities with the other available theoretical and experimental results to verify accuracies in our calculations. In addition, we also evaluate the lifetimes of the first two low-lying states of the ions using the above matrix elements. Graphical representations of the dispersion coefficients versus R are given among all the alkaline ions with Rb.

I. INTRODUCTION

Advancements in the simultaneous trapping and cooling of both ions and atoms in a hybrid trap [1,2] have resulted in a significant upsurge in the precise description of the atom-ion interactions. This new development of using hybrid traps in which neutral atoms and ions are confined together leads to the search for many exotic phenomena in the quantum information science and condensed-matter related fields [3]. Interaction between these systems can be described as the special case of the van der Waal long-range forces caused due to the fluctuating dipole moments of the systems [4]. These interactions can enable many chemical reactions like charge-exchange and molecule formations at the single-particle level; hence better understanding of these interactions is very useful in a number of studies such as explaining the underlying reasons for various quantum phase transitions [5], improvising quantum computing techniques [6], establishing sustained atom-ion sympathetic cooling mechanisms [7,8], designing ultracold superchemistry [9], studying the physics of impurities in the Bose gases [10,11], and interpreting cold atom collision processes [8].

Cotrapping of atoms and ions has several applications. Observations of the scattering between the atoms and the ions at the low-energy scale have been reported by a number of groups [12–14]. Early studies on the properties of the mixed atom-ion systems were reported by Côté and his coworkers in order to investigate the ultracold atom-ion collision dynamics and charge transportation processes and to realize possible formation of the combined stable system [15]. Recently, Härter and Denschlag observed that the elastic-scattering cross section of an atom-ion system depends on the collisional energy in the semiclassical regime and favors scattering at small angles [3]. Furthermore, the results of an atom-ion scattering event have been utilized to develop a novel and effective method to compensate excessive ion micromotion in a trap [16]. Although there have been attempts to study the atom-ion interactions in the past, the reported results were not very accurate. Due to the experimental advancements in the atom-ion trapping experiments, it is imperative to provide more accurate description of these potentials to infer important signatures of new physics. Owing to the simplified and well-understood structures of the alkali-metal atoms and alkaline-earth ions, they seem to be the natural choices and of immense interest for experimental investigations [17], for which we intend to carry out accurate theoretical studies of the long-range atom-ion interactions among these systems. In this work, we particularly undertake the Li, Na, K, and Rb alkali-metal atoms and the Ca^+, Sr^+, Ba^+, and Ra^+ alkaline-earth ions to estimate their long-range interactions.

Determination of the van der Waal coefficients of the atom-ion interactions requires evaluation of the dynamic dipole, quadrupole, and octupole polarizabilities at imaginary frequencies [18]. We evaluate these polarizabilities by using dominant contributing matrix elements and experimental energies in a sum-over-states approach. These transition matrix elements are extracted either from the measurements of the lifetimes and the static dipole polarizabilities of the atomic states or using a relativistic coupled-cluster (RCC) method. Other contributions such as from the core and core-valence correlations, which cannot be estimated using the sum-over-states approach, are estimated using other suitable many-body methods. Unless stated otherwise, we use atomic units (a.u.) throughout this paper.

---

*Email: arorabindiya@gmail.com
†Email: bijaya@prl.res.in

II. EVALUATION OF MULTIPOLAR POLARIZABILITIES

The dynamic dipole ($E1$) and quadrupole ($E2$) polarizabilities of the atomic systems with an imaginary frequency $\iota\omega$ are given by

$$\alpha_k(\iota\omega) = -\sum_{I \neq n} \frac{(E_n - E_I)|\langle\Psi_n|O_k|\Psi_I\rangle|^2}{(E_n - E_I)^2 + \omega^2}, \qquad (1)$$

where n is the principal quantum number of the ground state of the respective system, I represents all possible allowed intermediate states, $k = 1$ and $O_1 \equiv D = |e|r$ for the dipole polarizability (α_1), $k = 2$ and $O_2 \equiv Q = \frac{|e|}{2}(3z^2 - r^2)$ for the quadrupole polarizability (α_2), and $k = 3$ and $O_2 \equiv Q = |e|(r^3)$ for the octupole polarizability (α_3). For the *ab initio* evaluation of these quantities, one can express them as

$$\alpha_k(\iota\omega) = \langle\Psi_n|O_k|\Psi_n^-\rangle + \langle\Psi_n^+|O_k|\Psi_n\rangle \qquad (2)$$

with $|\Psi_n^\pm\rangle = \sum_{I \neq n}|\Psi_I\rangle\frac{\langle\Psi_I|O_k|\Psi_n\rangle}{(E_I - E_n)\pm i\omega}$, which can be treated as analogous to the first-order wave function with respect to the ground-state wave function $|\Psi_n\rangle$ due to the operator D. However, it is complicated to obtain these wave functions using sophisticated many-body methods like RCC owing to the presence of the imaginary factor in the denominator. Alternatively, we try to determine the ground- and singly excited-state wave functions of these systems using the following procedure. Indeed these states can be treated as a closed-shell configuration with a respective valence electron in the outermost orbital. We, therefore, calculate the Dirac-Fock (DF) wave function ($|\Phi_0\rangle$) for the closed-shell configuration first and then define the DF wave function of the ground or singly excited states of the considered systems by appending the valence orbital (v) to the DF wave function of the closed shell as $|\Phi_v\rangle = a_v^\dagger|\Phi_0\rangle$. The exact atomic wave functions of these states can now be evaluated by considering the correlations among the electrons within $|\Phi_0\rangle$ referred to as core correlation, correlations seen by the valence and core electrons of $|\Phi_v\rangle$ termed valence correlation, and correlations between the core electrons with the valence electron v named the core-valence contributions. Using the wave operator formalism, we can write these wave functions accounting for the above correlations independently as

$$|\Psi_v\rangle = a_v^\dagger\Omega_c|\Phi_0\rangle + \Omega_{cv}|\Phi_v\rangle + \Omega_v|\Phi_v\rangle, \qquad (3)$$

where Ω_c, Ω_{cv}, and Ω_v are known as the wave operators for the core, core-valence, and valence correlations, respectively.

With the above prescription, the square of the matrix element of O_k from Eq. (1) can be expressed as

$$\begin{aligned}
\langle\Psi_v|O_k|\Psi_I\rangle^2 &= \langle\Psi_v|O_k|\Psi_I\rangle\langle\Psi_I|O_k|\Psi_v\rangle \\
&= \langle\Phi_0|\Omega_c^\dagger O_k[\Omega_I\Omega_I^\dagger + \Omega_{cI}\Omega_{cI}^\dagger]O_k\Omega_c|\Phi_0\rangle \\
&\quad + \langle\Phi_v|\Omega_v^\dagger O_k[\Omega_{cI}\Omega_{cI}^\dagger + \Omega_I\Omega_I^\dagger]O_k\Omega_v|\Phi_v\rangle \\
&\quad + \langle\Phi_v|\Omega_v^\dagger O_k\Omega_c\Omega_c^\dagger O_k\Omega_v|\Phi_v\rangle \\
&\quad + \langle\Phi_I|\Omega_{cI}^\dagger O_k\Omega_c\Omega_c^\dagger O_k\Omega_{cv}|\Phi_v\rangle, \qquad (4)
\end{aligned}$$

where we have used the generalized Wick theorem to assemble different terms and assumed all the operators are in normal ordered form so that only the connected terms survive. For brevity, we categorize the first term as core (c), the next

two terms as valence (v), and the last term as core-valence (cv) contributions, for which we can now write the total polarizability as

$$\alpha_k = \alpha_k^c + \alpha_k^v + \alpha_k^{cv}, \qquad (5)$$

for the notations α_k^c, α_k^v, and α_k^{cv} corresponding to the above-mentioned three correlation contributions, respectively.

It is possible to evaluate dominant contributions to α_k^v by calculating many low-lying singly excited states $|\Psi_I\rangle$ of the considered systems by expressing them as

$$\begin{aligned}
\alpha_k^v(\iota\omega) = {}& \frac{2}{(2k+1)(2J_n+1)} \\
&\times \sum_{I \neq n}^{(')} \frac{(E_n - E_I)|\langle\Psi_n||O_k||\Psi_I\rangle|^2}{(E_n - E_I)^2 + \omega^2}, \qquad (6)
\end{aligned}$$

where $\langle\Psi_n||O_k||\Psi_I\rangle$ is the reduced matrix element of O_k and the symbol $(')$ in the summation implies that only the excited states are included in the sum. In order to determine the $E1$ and $E2$ matrix elements between the ground-state wave function $|\Psi_n\rangle$ and the excited-state wave function $|\Psi_I\rangle$, we express them in a general form as $|\Psi_v\rangle$ with a common core and for a valence orbital v representing either n or I, which in the Fock-space RCC formalism is defined as

$$|\Psi_v\rangle = e^T\{1 + S_v\}|\Phi_v\rangle. \qquad (7)$$

Here the operator T and S_v excite core electrons and the valence electron along with the core electrons due to the electron correlations. We consider all possible single and double excitations with the important valence triple excitations in our calculations [referred to as the CCSD(T) method in the literature] within a sufficiently large configuration space. From practical limitation, we calculate as many $|\Psi_I\rangle$ states as possible for the estimation of their contributions to α_k^v and refer to them as the main contribution (α^{vm}). Contributions from the higher excited states, which are relatively small, are estimated using the following equation at the DF approximation:

$$\alpha_k^{vt}(\iota\omega) = \langle\Psi_n|O_k|\Psi_n^{(1)}\rangle, \qquad (8)$$

where $|\Psi_n^{(1)}\rangle$ is obtained by solving the inhomogeneous equation for the effective Hamiltonian $H_{\text{eff}} = (H - E_n)O_k$ as

$$[(H - E_n)^2 + \omega^2]|\Psi_n^{(1)}\rangle = -H_{\text{eff}}|\Psi_n\rangle \qquad (9)$$

and given as the tail contribution (α_k^{vt}). We also obtain the α_k^{cv} contributions using the same procedure as has been described by the above equation. Nonetheless, the α_k^c contributions may not be small enough to be estimated using the DF method, for which we employ the random-phase approximation (RPA) to solve for the core configuration (denoted by subscript zero) with the similar logic as Eq. (9) by defining

$$\begin{aligned}
\big|\Psi_0^{(1)}\big\rangle &= \sum_\beta^\infty \sum_{p,a} \Omega_{a \to p}^{(\beta,1)}|\Phi_0\rangle \\
&= \sum_{\beta=1}^\infty \sum_{pq,ab} \left\{ \frac{[\langle pb|\frac{1}{r_{12}}|aq\rangle - \langle pb|\frac{1}{r_{12}}|qa\rangle]\Omega_{b \to q}^{(\beta-1,1)}}{(\epsilon_p - \epsilon_a)^2 + \omega^2} \right.
\end{aligned}$$

$$+ \frac{\Omega_{b \to q}^{(\beta-1,1)^\dagger} \left[\langle pq | \frac{1}{r_{12}} | ab \rangle - \langle pq | \frac{1}{r_{12}} | ba \rangle \right]}{(\epsilon_p - \epsilon_a)^2 + \omega^2} \Bigg\}$$
$$\times (\epsilon_p - \epsilon_a) | \Phi_0 \rangle, \tag{10}$$

where $\Omega_{a \to p}^{(\beta,1)}$ is the wave operator that excites an occupied orbital a of $|\Phi_0\rangle$ to a virtual orbital p which alternatively refers to a singly excited state with respect to $|\Phi_0\rangle$ with $\Omega_{a \to p}^{(0,1)} = \frac{\langle p | (\epsilon_p - \epsilon_a) O_k | a \rangle}{(\epsilon_p - \epsilon_a)^2 + \omega^2}$ for the single-particle orbital energies ϵ and the superscripts β and 1 representing the number of the Coulomb ($\frac{1}{r_{12}}$) and O_k operators, respectively.

III. ATOM-ION INTERACTION POTENTIALS

The long-range potential $V(R)$ between an electrically charged ion and a neutral atom in their ground states, with R as the internuclear distance, is divided in terms of the induced and dispersed interactions among the multipole moments as [19,20]

$$V(R) = V_{\text{ind}}(R) + V_{\text{dis}}(R), \tag{11}$$

where $V_{\text{ind}}(R)$ and $V_{\text{dis}}(R)$ are known as the induced and dispersion potentials, respectively. It can be noted that a small contribution coming from the exchange potential [19] has been neglected in the above expression. The induced part of this potential occurs due to polarization from the attractive interaction of the permanent multipole of the ion with the induced multipole of the atom due to the ion and is expressed in terms of the induction coefficients (c_{2n}) as [19,20]

$$V_{\text{ind}}(R) = -Q^2 \sum_{n=1}^{\infty} c_{2n}/R^{2n}, \tag{12}$$

where Q is the charge of the ion and the negative sign indicates that the force is attractive in nature. In the above equation, the term R^{-2}, which corresponds to the charge-dipole interaction, vanishes for the interaction of an ion with a neutral atom. The second term inside the summation, corresponding to $n = 2$, is a spherically symmetric term arising due to the ion-induced dipole potential and is given as c_4/R^4 with $c_4 = \alpha_1/2$ for the static dipole polarizability α_1 of the atom. This term originates due to the electric field created by the ion, which induces an electric dipole moment in the neutral atom. This part of the potential is independent of the electronic state of the ion, but varies with the electronic state of the atom due to the dependencies on their α_1. Once the c_4 coefficients are known, one can also calculate the characteristic length scale (R^*), the effective range of the polarization potential, by equating the potential to the kinetic energy as $R^* = \sqrt{2\mu c_4}$ [3,21]. The characteristic energy scale is further expressed in terms of R^* as $E^* = 1/2\mu R^{*2}$. Here $\mu = (m_{\text{ion}})(m_{\text{at}})/(m_{\text{ion}} + m_{\text{at}})$ is the reduced mass of the system for the mass of the ion m_{ion} and mass of the atom m_{at}. The next term with powers of R^{-6} in the general expression [Eq. (12)] appears due to the instantaneous fluctuating dipole moments between the atoms and can be expressed as $\frac{c_6}{R^6}$ with $c_6 = \alpha_2/2$ for the quadrupole polarizability α_2 of the atom.

For the atom and ion being in their respective ground states, the expression for the dispersion interaction potential is given

by [15,22]

$$V_{\text{dis}}(R) = -\frac{C_6}{R^6} - \frac{C_8}{R^8} - \frac{C_{10}}{R^{10}} \cdots . \tag{13}$$

The coefficients C_6, C_8, C_{10}, ..., etc., emerge from the instantaneous dipole-dipole, dipole-quadrupole, dipole-octupole, quadrupole-quadrupole, etc., interactions and are known as the dispersion coefficients.

In Eq. (13), the dispersion coefficients C_6^{AB}, C_8^{AB}, and C_{10}^{AB} between an atom A and an ion B can be estimated using the expressions given as [23]

$$C_6^{AB} = \frac{3}{\pi} \int_0^\infty d\omega \, \alpha_1^A(\iota\omega) \alpha_1^B(\iota\omega), \tag{14}$$

$$C_8^{AB} = \frac{15}{2\pi} \int_0^\infty d\omega \, \alpha_1^A(\iota\omega) \alpha_2^B(\iota\omega)$$
$$+ \frac{15}{2\pi} \int_0^\infty d\omega \, \alpha_2^A(\iota\omega) \alpha_1^B(\iota\omega), \tag{15}$$

$$C_{10}^{AB} = \frac{14}{\pi} \int_0^\infty d\omega \, \alpha_1^A(\iota\omega) \alpha_3^B(\iota\omega) + \frac{14}{\pi} \int_0^\infty d\omega \, \alpha_3^A(\iota\omega) \alpha_1^B(\iota\omega)$$
$$+ \frac{35}{\pi} \int_0^\infty d\omega \, \alpha_2^A(\iota\omega) \alpha_2^B(\iota\omega). \tag{16}$$

Here $\alpha_1^A(\iota\omega)$ and $\alpha_1^B(\iota\omega)$ are the electric dipole, $\alpha_2^A(\iota\omega)$ and $\alpha_2^B(\iota\omega)$ are the quadrupole, and $\alpha_3^A(\iota\omega)$ and $\alpha_3^B(\iota\omega)$ are the octupole atomic and ionic dynamic polarizabilities at imaginary frequencies, respectively. For numerical integration of the product of these polarizabilities, we use an exponential grid of the following form:

$$r(i) = r_0[\exp^{(i-1)h} - 1]. \tag{17}$$

Here grid size h is 0.03125, r_0 is 0.0005, and the total number of grids is 500. In our earlier works, we had determined dynamic dipole polarizabilities of the alkali-metal atoms for a sufficiently large number of imaginary frequencies very precisely [32,33]. In the present work, we further determine the quadrupole and octupole polarizabilities for the alkaline-earth ions as well as for the alkali-metal atoms in order to determine the van der Waals coefficients accurately. In order to determine $E1$ and $E2$ polarizabilities in the considered systems which have one valence electron each outside the closed core, we use the CCSD method and the calculations for $E3$ polarizabilities are carried out by the DHF method, respectively. Moreover, we also determine the lifetimes of the first excited np states of the alkaline-earth ions and compare them with the available experimental and other precise calculations in order to test the accuracies of the dipole matrix elements of the transitions that are predominantly contributing in the determination of the dipole polarizabilities of the considered ions.

IV. RESULTS AND DISCUSSION

A. Calculation of lifetimes of the np states

As a test of accuracy of our calculated principal matrix elements which are going to contribute predominantly to the α_1 results of the alkaline-earth ions, we estimate the lifetimes (τ) of the np states using these matrix elements with n being the principal quantum number of the ground states of the

TABLE I. Contributions to the lifetimes of the $np_{1/2}$ and $np_{3/2}$ states of the alkaline Ca^+, Sr^+, Ba^+, and Ra^+ ions. The transition rates (A) are given in 10^6 s^{-1} and the lifetimes (τ) are given in ns.

Ca+				Sr+			
$4p_{1/2}$		$4p_{3/2}$		$5p_{1/2}$		$5p_{3/2}$	
$A(4p_{1/2} \rightarrow 4s_{1/2})$	137.24	$A(4p_{3/2} \rightarrow 4s_{1/2})$	141.12	$A(5p_{1/2} \rightarrow 5s_{1/2})$	130.1	$A(5p_{3/2} \rightarrow 5s_{1/2})$	144.12
$A(4p_{1/2} \rightarrow 3d_{3/2})$	10.81	$A(4p_{3/2} \rightarrow 3d_{3/2})$	1.14	$A(5p_{1/2} \rightarrow 4d_{3/2})$	9.22	$A(5p_{3/2} \rightarrow 4d_{3/2})$	1.17
$\Sigma\,A$	148.05	$A(4p_{3/2} \rightarrow 3d_{5/2})$	10.17	$\Sigma\,A$	139.32	$A(4p_{3/2} \rightarrow 3d_{5/2})$	9.89
		$\Sigma\,A$	152.37			$\Sigma\,A$	155.18
$\tau(4p_{1/2})$		$\tau(4p_{3/2})$		$\tau(5p_{1/2})$		$\tau(5p_{3/2})$	
Present	6.75		6.55	Present	7.16		6.44
Others	6.88 [24]		6.69 [24]	Others	7.376 [25]		6.653 [25]
Expt.	6.96(35) [26]		6.71(25) [26]	Expt.	7.35(30) [27]		6.53(20) [27]
				Expt.	7.39(7) [28]		6.63(7) [28]
Ba+				Ra+			
$6p_{1/2}$		$6p_{3/2}$		$7p_{1/2}$		$7p_{3/2}$	
$A(6p_{1/2} \rightarrow 6s_{1/2})$	95.13	$A(6p_{3/2} \rightarrow 6s_{1/2})$	119.88	$A(7p_{1/2} \rightarrow 7s_{1/2})$	106.08	$A(7p_{3/2} \rightarrow 7s_{1/2})$	187.95
$A(6p_{1/2} \rightarrow 5d_{3/2})$	35.70	$A(6p_{3/2} \rightarrow 5d_{3/2})$	4.53	$A(7p_{1/2} \rightarrow 6d_{3/2})$	10.56	$A(7p_{3/2} \rightarrow 6d_{3/2})$	3.38
$\Sigma\,A$	130.83	$A(6p_{3/2} \rightarrow 5d_{5/2})$	35.30	$\Sigma\,A$	116.64	$A(7p_{3/2} \rightarrow 6d_{5/2})$	22.89
		$\Sigma\,A$	159.72			$\Sigma\,A$	214.23
$\tau(6p_{1/2})$		$\tau(6p_{3/2})$		$\tau(7p_{1/2})$		$\tau(7p_{3/2})$	
Present	7.64		6.26	Present	8.57		4.66
Others	7.83 [29]		6.27 [29]	Others	8.72 [30]		4.73 [30]
Expt.	7.74(40) [27]		6.27(25) [27]				

respective ions and compare them with the experimental and other high-precision calculations. The contributions to the lifetimes of the $np_{1/2}$ and $np_{3/2}$ states are given in Table I and are estimated considering only the dominant $E1$ transition probabilities (A), which are evaluated (in s^{-1}) using the formula

$$A_{ij}^{E1} = \frac{2.02613 \times 10^{15}}{\lambda^3} \frac{|\langle i \| D \| j \rangle|^2}{2j_i + 1},\qquad(18)$$

where λ is the wavelength of the transition in Å and $|\langle i \| D \| j \rangle|^2$ is the reduced $E1$ matrix elements in a.u. Since our aim is to know the accuracies of the $E1$ matrix elements alone, we use the experimental λ values in these calculations. As can be seen from the table, the experimental results have large error bars [26], however our calculated values are compared with other high-precision calculations [24] in Ca^+. Pulse laser excitation measurements of the lifetimes for $4p_{1/2}$ and $4p_{3/2}$ levels are reported by Ansbacher *et al.* [26]. Safronova and Safronova presented precision $4p_{1/2}$ and $4p_{3/2}$ lifetime measurements in Ref. [24]. Precision measurement of the lifetime of Sr^+ is presented by Jiang *et al.* in Ref. [25]. Lifetimes of the $5p_{1/2,3/2}$ states of Sr^+ and the $6p_{1/2,3/2}$ states of Ba^+ are observed by Gallagher [27] using the Hanle-effect method with the optical excitations from the ground states. These values are 7.35(0.3) and 6.53(0.2) ns for the $5p_{1/2}$ and $5p_{3/2}$ states of Sr^+, respectively, which are later improved by Pinnington *et al.* [28]. Our results are close to these values and the used $E1$ matrix elements can be used further to estimate α_1 of Sr^+ within a reasonably accuracy. Similarly, the experimental lifetimes of the $6p_{1/2,3/2}$ states of Ba^+ are reported as $\tau(6p_{1/2}) = 7.74(0.4)$ ns and $\tau(6p_{3/2}) = 6.27(0.25)$ ns [27] and other theoretical values are given as $\tau(6p_{1/2}) = 7.83$ ns and $\tau(6p_{3/2}) = 6.27$ ns [29], which are in

good agreement with our results, suggesting that when the corresponding $E1$ matrix elements are used we will be able to achieve a high-accuracy α_1 value in Ba^+. There are no experimental results available for the lifetimes of the $7p_{1/2,3/2}$ states of Ra^+, however our results are in close agreement with other calculations by Pal *et al.* [30]. Therefore, the resulting α_1 values in all the above-discussed ions will be reliable and hence we expect to attain accurate values of the dispersion coefficients when α_1 values are used from our calculations.

B. Calculation of c_4 coefficients

In Table III, we present the static dipole polarizabilities of the alkali-metal atoms that were reported by us in Ref. [44] and compare with the earlier theoretical and experimental results. The details of the calculations are presented in Ref. [44] and we do not repeat them here again. The reported values of α_1 are slightly different than Ref. [44], since the core contributions from the DF method are replaced by the RPA values here. From the comparison between the measured and calculated results, as shown in the table, it is clear that our static polarizabilities are in close agreement with the experimental and theoretical values, which gives us confidence in using these values for the calculation of the c_4 coefficients as 82.1, 81.2, 144.9, and 156.0 a.u. in the Li, Na, K, and Rb atoms, respectively. Using these c_4 values, we further obtain a range of potential R^* and compare it with the values obtained by Idziaszek *et al.* [31] and Doerk *et al.* [21], as shown in Table II. These authors have applied the multichannel quantum defect theory to describe the range of the atom-ion systems. On comparison, we observe that our calculated values are close to the values tabulated in these references. As expected, the effective length scale of the atom-ion potential is much more long ranged than the interaction

TABLE II. Calculated values of effective range R^* of the atom-ion interaction potentials and energy scale for the given atom-ion system. The results are compared with other theoretical works wherever available.

	R^* (in a.u.)	$E^* \times 10^{11}$ (in a.u.)		R^* (in a.u.)	$E^* \times 10^{11}$ (in a.u.)
Li-Ca$^+$	1336	0.09	K-Ca$^+$	3231	1.88
Li-Sr$^+$	1393	0.11	K-Sr$^+$	3779	3.52
Li-Ba$^+$	1412	0.12	K-Ba$^+$	3999	4.41
Li-Ra$^+$	1423	0.13	K-Ra$^+$	4193	5.33
Na-Ca$^+$	2079	0.57	Rb-Ca$^+$	3991	3.95
	2081 [21,31]			3989 [21,31]	
Na-Sr$^+$	2324	0.89	Rb-Sr$^+$	5042	10.03
Na-Ba$^+$	2412	1.04	Rb-Ba$^+$	5545	14.6
Na-Ra$^+$	2486	1.17		5544 [21,31]	
			Rb-Ra$^+$	6042	20.57

between two neutral atoms. In the same table we also present the characteristic energies for their direct applications in future experimental studies.

C. Calculation of c_6 coefficients

In order to obtain the c_6 coefficients, we first carry out systematic calculations of the quadrupole polarizabilities of the Li, Na, K, and Rb atoms. As given in Table III, terms α_2^c, α_2^v, and α_2^{VC} summarize the contributions to the quadrupole polarizabilities from the core, valence, and valence-core correlation terms. Here the matrix elements of the first five $ns-n'd_{5/2}$ transitions in each alkali-metal atom are included into the main term α_2^{vm} calculations, where n is the principal quantum number of the ground state of the respective atom. For example, in the Na atom, $3s$ to $(3-7)d_{5/2}$ transition $E2$ matrix elements are included in the main polarizability calculations. Moreover, for the Li atom calculation, we have included two more transitions $2s-8d_{5/2}$ and $2s-9d_{5/2}$ in the main polarizability calculations. In the above table, we compare

our results with the predictions by other studies. For the Li atom, an accurate value of the quadrupole polarizability is obtained as 1424 a.u. by Porsev and Derevianko [41] using the relativistic many-body calculations. Our result 1426 a.u. is in very good agreement with this value. Theoretical values of the quadrupole polarizability of the Na atom were given by the group of Spelsberg *et al.* [42] and the group of Makarov *et al.* [22] as 1879 and 1902 a.u., respectively, and are also in close agreement with our value of 1895 a.u. The group of Makarov *et al.* has calculated the quadrupole polarizability of Na using the Möller Plesset second-order perturbation theory with an extended Gaussian basis. From the earlier studies, the results available to compare the polarizability values of the K and Rb atoms are 5000 and 6459 a.u. [43], calculated using a model potential method showing only small variations from our results 4947 and 6491 a.u., respectively. The comparisons, as given in Table III, reflect that our polarizabilities are reliable enough for the accurate determination of the c_6 results for the alkali-metal atoms. Our numerical calculations for the c_6 coefficients are 713, 947, 2474, and 3245 a.u. for the Li, Na, K, and Rb atoms, respectively.

D. Calculations of dispersion coefficients

In Tables VI and VII we present the compiled values of contributions to the total dispersion coefficients between the alkali-metal atoms interacting with the alkaline ions. For the determination of the C_6 and C_8 dispersion coefficients, we perform the RCC calculations to obtain the dipole and quadrupole matrix elements for the evaluation of the required polarizabilities of the Ca$^+$, Sr$^+$, Ba$^+$, and Ra$^+$ ions. Tables IV and V summarize the contribution to dipole and quadrupole polarizabilities of alkaline-earth ions from core (α_c), valence-core (α_{VC}), and tail (α_{tail}) terms. The main contributions are listed separately along with the respective values of the matrix elements. For the main contributions, we use the combination of our CCSD(T) values of the matrix elements with the experimental energies. Several calculations of the ground-state polarizabilities of the alkaline-earth ions are

TABLE III. Calculated values of the static dipole and quadrupole polarizabilities along with the c_4 and c_6 coefficients for the Li, Na, K, and Rb alkali-metal atoms. Polarizability values are compared with the other available theoretical and experimental results. References are given in the square brackets and uncertainties are given in parentheses.

Polarizabilities	Li	Na	K	Rb
α_1^{vm}	162.5	161.9	284.3	309.1
α_1^c	0.2	0.9	5.5	9.1
α_1^{VC}	0.0	0.0	−0.1	−0.3
α_1^{tail}	1.2	0.08	0.06	0.11
α_1^{total} (Present)	164.1(6)	162.4(2)	289.8(6)	318.3(6)
α_1^{total} (Other)	164.112(1) [34]	162.9(6) [35]	289.3 [36]	315.7 [37]
α_1^{total} (Expt.)	164.2(1.1) [38]	162.1(8) [39]	290.58(1.42) [40]	318.79(1.42) [40]
c_4 coefficients	82.1(6)	81.2(2)	144.8(6)	159.9(6)
α_2^{vm}	1345	1780	4839	6244
α_2^c	∼0	2	16	35
α_2^{VC}	0	0	0	0
α_2^{tail}	81	113	94	211
α_2^{total} (Present)	1426(7)	1895(9)	4947(15)	6491(18)
α_2^{total} (Other)	1424 [41]	1879 [42], 1902 [22]	5000 [43]	6459 [43]
c_6 coefficients	713(7)	947(9)	2474(15)	3245(18)

TABLE IV. Individual contributions to α_1 of Ca$^+$, Sr$^+$, Ba$^+$, and Ra$^+$ alkaline-earth ions. Our results are also compared with other calculations and experimental values. References are given in the square brackets and uncertainties are given in parentheses.

Contributions	$E1$ amplitude	α_1	Contributions	$E1$ amplitude	α_1
		Ca$^+$			Sr$^+$
$4s_{1/2} \longrightarrow 4p_{1/2}$	2.913(7)	24.64(3)	$5s_{1/2} \longrightarrow 5p_{1/2}$	3.109(7)	29.81(4)
$4s_{1/2} \longrightarrow 5p_{1/2}$	0.068(8)	0.005	$5s_{1/2} \longrightarrow 6p_{1/2}$	0.022(6)	0.0006
$4s_{1/2} \longrightarrow 6p_{1/2}$	0.080(8)	0.006	$5s_{1/2} \longrightarrow 7p_{1/2}$	0.062(5)	0.004
$4s_{1/2} \longrightarrow 7p_{1/2}$	0.065(7)	0.004	$5s_{1/2} \longrightarrow 8p_{1/2}$	0.054(5)	0.003
$4s_{1/2} \longrightarrow 8p_{1/2}$	0.052(6)	0.002	$5s_{1/2} \longrightarrow 5p_{3/2}$	4.394(6)	57.61(6)
$4s_{1/2} \longrightarrow 9p_{1/2}$	0.041(6)	0.002	$5s_{1/2} \longrightarrow 6p_{3/2}$	0.037(4)	0.002
$4s_{1/2} \longrightarrow 4p_{3/2}$	4.120(1)	48.86(1)	$5s_{1/2} \longrightarrow 7p_{3/2}$	0.052(5)	0.003
$4s_{1/2} \longrightarrow 5p_{3/2}$	0.080(8)	0.008	$5s_{1/2} \longrightarrow 8p_{3/2}$	0.053(4)	0.003
$4s_{1/2} \longrightarrow 6p_{3/2}$	0.104(5)	0.011			
$4s_{1/2} \longrightarrow 7p_{3/2}$	0.087(4)	0.007			
$4s_{1/2} \longrightarrow 8p_{3/2}$	0.070(4)	0.004			
$4s_{1/2} \longrightarrow 9p_{3/2}$	0.055(4)	0.003			
α_c		3.25(1)	α_c		4.98(3)
α_{tail}		5.51×10^{-2}	α_{tail}		1.96×10^{-2}
α_{VC}		-8.85×10^{-2}	α_{VC}		-0.19
α_{total} (Present)		76.7(2)	α_{total} (Present)		92.2(2)
α_{total} (Other)		75.88 [45]	α_{total} (Other)		91.10 [45]
α_{total} (Other)		75.49 [20]	α_{total} (Other)		91.3(9) [25]
α_{total} (Other)		75.28 [50]	α_{total} (Expt.)		93.3(9) [47]
α_{total} (Other)		76.1(5) [24]			
α_{total} (Expt.)		75.3(4) [46]			
		Ba$^+$			Ra$^+$
$6s_{1/2} \longrightarrow 6p_{1/2}$	3.36(1)	40.763(8)	$7s_{1/2} \longrightarrow 7p_{1/2}$	3.28(2)	36.86(1)
$6s_{1/2} \longrightarrow 7p_{1/2}$	0.10(1)	0.0148	$7s_{1/2} \longrightarrow 8p_{1/2}$	0.04(4)	0.002
$6s_{1/2} \longrightarrow 8p_{1/2}$	0.11(5)	0.0157	$7s_{1/2} \longrightarrow 9p_{1/2}$	0.09(3)	0.009
$6s_{1/2} \longrightarrow 6p_{3/2}$	4.73(3)	74.56(4)	$7s_{1/2} \longrightarrow 7p_{3/2}$	4.54(2)	57.53(2)
$6s_{1/2} \longrightarrow 7p_{3/2}$	0.17(5)	0.04	$7s_{1/2} \longrightarrow 8p_{3/2}$	0.49(2)	0.335(1)
$6s_{1/2} \longrightarrow 8p_{3/2}$	0.11(5)	0.02	$7s_{1/2} \longrightarrow 9p_{3/2}$	0.30(2)	0.10
α_c		9.35(5)	α_c		11.66(5)
α_{tail}		1.66×10^{-2}	α_{tail}		0.15
α_{VC}		-0.38	α_{VC}		-0.74
α_{total} (Present)		124.4(5)	α_{total} (Present)		105.9(6)
α_{total} (Other)		123.07 [45]	α_{total} (Other)		105.37 [45]
α_{total} (Other)		126.2 [48]	α_{total} (Other)		106.5 [36]
α_{total} (Expt.)		123.88(5) [49]			

available using different methods. Similarly, a number of precise measurements of these quantities are also reported in the literature. We have compared our reported dipole polarizabilities results with the available theoretical and experimental values in Table IV. As can be seen from the table, Lim and Schwerdtfeger [45] listed the static dipole polarizabilities of all the considered alkaline-earth ions, which are in very close agreement with our values. Their values are predicted using the RCC calculations in the finite field gradient technique together with the optimized Gaussian-type basis set. However, use of a sum-over-states approach allowed us to use experimental data wherever available, which we believe can minimize the uncertainties in the results, and hence they are more accurate in our case. Experimental spectral analysis of the dipole polarizability value of the Ca$^+$ ion is observed by Chang [46] and is in very good agreement with our calculated value. Another method used by Safronova and Safronova is the relativistic all-order single double where all the single, double, and partial triple excitations of the wave function are included to all orders of the perturbation theory to calculate the polarizability of Ca$^+$ [24]. As expected, our results of the calculated electric dipole static polarizability of Ca$^+$ lie within the error bars of the results quoted by Ref. [24]. As seen from the given table, the calculated values of these quantities by Mitroy and Zhang [20], which are evaluated by diagonalizing the semiempirical Hamiltonian in a large dimension single electron basis, are also in agreement with our values. However, we would like to emphasize that our results are more accurate since in our method core correlations are accounted for through the all-order RPA. The most recent dipole polarizability of Ca$^+$ available for the comparison, calculated through the DFCP method, is 75.28 a.u. [50]. The estimate of 93.3 a.u. [51] for the ground-state polarizability of the Sr$^+$ ion, derived by combining the experimental data given by the group of Barklem and OMara [47] with the oscillator strength sums, has a considerable discrepancy with our present results. There have also been calculations using the Dirac-Fock plus core polarization (DFCP) model. In contrast,

TABLE V. Individual contributions to α_2 of Ca^+, Sr^+, Ba^+, and Ra^+ alkaline-earth ions. Our results are also compared with other calculations and experimental values. References are given in the square brackets and uncertainties are given in parentheses.

Contributions	$E2$ amplitude	α_2	Contributions	$E2$ amplitude	α_2
	Ca^+			Sr^+	
$4s_{1/2} \longrightarrow 3d_{3/2}$	8.12(5)	212(3)	$5s_{1/2} \longrightarrow 4d_{3/2}$	11.25(7)	382(5)
$4s_{1/2} \longrightarrow 4d_{3/2}$	12.51(8)	121(2)	$5s_{1/2} \longrightarrow 5d_{3/2}$	12.87(8)	136(2)
$4s_{1/2} \longrightarrow 5d_{3/2}$	3.89(4)	9.1(2)	$5s_{1/2} \longrightarrow 6d_{3/2}$	5.00(5)	16.2(3)
$4s_{1/2} \longrightarrow 6d_{3/2}$	2.44(6)	16.2(4)	$5s_{1/2} \longrightarrow 7d_{3/2}$	3.11(4)	5.7(1)
$4s_{1/2} \longrightarrow 3d_{5/2}$	9.97(6)	318(3)	$5s_{1/2} \longrightarrow 4d_{5/2}$	13.91(8)	572(6)
$4s_{1/2} \longrightarrow 4d_{5/2}$	15.30(9)	181(2)	$5s_{1/2} \longrightarrow 5d_{5/2}$	15.64(9)	201(2)
$4s_{1/2} \longrightarrow 5d_{5/2}$	4.75(5)	13.6(3)	$5s_{1/2} \longrightarrow 6d_{5/2}$	5.97(6)	23.3(4)
$4s_{1/2} \longrightarrow 6d_{5/2}$	2.98(6)	24.2(4)	$5s_{1/2} \longrightarrow 7d_{5/2}$	3.76(4)	8.3(1)
α_c		6.77(8)	α_c		9.34(9)
α_{tail}		5.36(5)	α_{tail}		6.35(8)
α_{VC}		0.0	α_{VC}		-1.7×10^{-8}
α_{total} (Present)		906(5)	α_{total} (Present)		1361(9)
α_{total} (Other)		882.43 [50]	α_{total} (Other)		1346 [51]
α_{total} (Other)		875.1 [20]			
α_{total} (Other)		871(4) [24]			
	Ba^+			Ra^+	
$6s_{1/2} \longrightarrow 5d_{3/2}$	12.76(5)	1466(11)	$7s_{1/2} \longrightarrow 6d_{3/2}$	14.997(30)	816(32)
$6s_{1/2} \longrightarrow 6d_{3/2}$	16.58(12)	262(4)	$7s_{1/2} \longrightarrow 7d_{3/2}$	13.977(45)	175(11)
$6s_{1/2} \longrightarrow 7d_{3/2}$	5.727(7)	24.07(6)	$7s_{1/2} \longrightarrow 8d_{3/2}$	5.646(15)	22.6(1)
$6s_{1/2} \longrightarrow 8d_{3/2}$	4.036(5)	10.72(3)	$7s_{1/2} \longrightarrow 9d_{3/2}$	3.320(12)	7.08(5)
$6s_{1/2} \longrightarrow 5d_{5/2}$	15.99(8)	1978(20)	$7s_{1/2} \longrightarrow 10d_{3/2}$	2.234(14)	3.04(3)
$6s_{1/2} \longrightarrow 6d_{5/2}$	19.99(20)	380(8)	$7s_{1/2} \longrightarrow 11d_{3/2}$	1.753(12)	1.81(2)
$6s_{1/2} \longrightarrow 7d_{5/2}$	7.024(9)	36.1(1)	$7s_{1/2} \longrightarrow 6d_{5/2}$	19.176(30)	1174(36)
$6s_{1/2} \longrightarrow 8d_{5/2}$	5.022(5)	16.59(3)	$7s_{1/2} \longrightarrow 7d_{5/2}$	16.175(50)	233.2(14)
			$7s_{1/2} \longrightarrow 8d_{5/2}$	6.787(12)	32.62(2)
			$7s_{1/2} \longrightarrow 9d_{5/2}$	4.050(13)	10.52(6)
			$7s_{1/2} \longrightarrow 10d_{5/2}$	2.749(12)	4.59(4)
			$7s_{1/2} \longrightarrow 11d_{5/2}$	2.195(10)	2.83(2)
α_c		46(2)	α_c		68(1)
α_{tail}		50(10)	α_{tail}		39.6(5)
α_{VC}		-0.001	α_{VC}		-3.46×10^{-4}
α_{total} (Present)		4270(27)	α_{total} (Present)		2592(49)
α_{total} (Other)		4182(34) [29]	α_{total} (Other)		2533(26) [30]
α_{total} (Expt.)		4420(250) [49]			

our values match very well with the calculations of Jiang *et al.* [25], who have used the relativistic all-order method to calculate the polarizabilities of the Sr^+ ion. It would be interesting to see the validity of these results when the new measurement of the ground-state polarizability for this ion becomes available. The polarizability value of the Ba^+ ion was calculated by Miadokova *et al.* [48] using the relativistic basis set in the Douglas-Kroll no-pair approximation and has a 2% discrepancy from the high-precision measurements performed by Snow and Lundeen [49]. This high-precision measurement was achieved by a novel technique based on the resonant excitation Stark ionization spectroscopy microwave technique. We find that our results are also in better agreement with this experimental value. In addition we have calculated the quadrupole polarizability for the heaviest alkali-metal ion Ra^+ using the above-mentioned CCSD(T) method. The most challenging part of this ion is that there is no experimental result available for the dipole polarizability of Ra^+ to compare with our result. However, Safronova *et al.* [36] have evaluated this result using the relativistic all-order method. The group of

Lim and Schwerdtfeger [45] also calculates the polarizability result of Ra^+ based on the CCSD(T) method using the scalar relativistic Douglas-Kroll operator, which is in agreement with our result. It can be noticed from Table IV that the polarizability value for Ra^+ is lower by 18% in comparison to Ba^+, which is similar to the trend observed by Ref. [45]. In fact their value in the case of Ra^+ is 17% lower than the value for Ba^+. They attribute this reduction in polarizability of Ra^+ to the dominating contribution of relativistic effects over correlation effects.

Absolute values of the $E2$ matrix elements with their uncertainties are listed in Table V. These matrix elements were also calculated by us earlier using the same CCSD(T) method [53,54]. It is evident from Table V that an overwhelmingly dominant contribution to the total values in the case of quadrupole polarizability values is due to the terms containing $ns_{1/2}$ to $(n-1)d_{3/2}$ and $(n-1)d_{3/2}$ matrix elements with n taking the values 4,5,6, and 7 for Ca^+, Sr^+, Ba^+, and Ra^+ ions, respectively. The ground-state quadrupole polarizability in the case of the Ca^+ ion is 906 a.u., which is about 1%

TABLE VI. Total values of the C_6 coefficients for the interaction between the 16 combinations of alkali-metal atoms and the alkaline ions. Their breakdown contributions labeled as C_6^v, C_6^c, C_6^{VC}, and C_6^{CT} are obtained by using the corresponding polarizability contributions. We have given the references in square brackets and uncertainties in parentheses.

	Individual contributions to the C_6 coefficients					
	C_6^v	C_6^c	$C_6^{VC} \times 10^{-2}$	C_6^{CT}	Total (C_6)	Total (C_6) [52]
Li-Ca$^+$	768.4	1.0	0.0	67.35	837(6)	824
Li-Sr$^+$	898.1	1.5	0.0	108.4	1008(6)	981
Li-Ba$^+$	1127.1	2.6	0.0	184.8	1315(8)	1275
Li-Ra$^+$	974.3	3.2	0.0	228.9	1206(8)	
Na-Ca$^+$	826.4	4.6	0.22	69.7	901(3)	889
Na-Sr$^+$	964.6	7.4	0.43	113.6	1085(3)	1059
Na-Ba$^+$	1205.7	12.4	0.74	195.6	1414(5)	1373
Na-Ra$^+$	1046.5	15.1	1.3	244.3	1305(6)	
K-Ca$^+$	1231.4	19.6	1.0	141.0	1392(6)	1372
K-Sr$^+$	1441.5	31.6	2.0	207.1	1680(6)	1636
K-Ba$^+$	1816.2	53.0	3.6	328.3	2197(8)	2130
K-Ra$^+$	1563.4	66.1	6.5	389.9	2019(8)	
Rb-Ca$^+$	1312.9	29.6	1.8	184.8	1527(6)	1506
Rb-Sr$^+$	1537.3	48.4	3.8	259.5	1845(6)	1798
Rb-Ba$^+$	1938.1	81.5	6.7	394.5	2414(8)	2340
Rb-Ra$^+$	1667.2	101.6	0.1	455.5	2224(8)	

larger than the value 875.1 a.u. as obtained by Ref. [20]. Also, we find a large discrepancy in the results of calculated polarizability by us and Safronova and Safronova [24] given as 871(4) a.u. for Ca$^+$. However, our value is only 3% larger than the recent calculated value of Ref. [50]. The quadrupole polarizability value for Sr$^+$ is 1366(9) a.u., which differs by 2% from the results reported in Ref. [51], in which the authors have evaluated the polarizability by diagonalizing a semiempirical Hamiltonian in a large dimension single-electron basis. Our recommended value for the ground-state quadrupole polarizability of Ba$^+$ is in agreement within the corresponding uncertainties with the most recent experimental

work [49]. However, the analysis of Iskrenova-Tchoukova and Safronova [29] based on the relativistic all-order method also gives a consistent result. For the heavier alkaline ion Ra$^+$, the only useful data are the results of Pal *et al.* The calculations of Ref. [30] are carried out by using the high-precision relativistic all-order method, which includes all single and double excitations of the Dirac-Fock wave functions.

Having compared all our polarizability results, we are now in a state to justify the fact that since our static polarizability values are very accurate we anticipate similar accuracies for the calculated dynamic polarizabilities using our method and that our method can be used reliably for the

TABLE VII. Total values of the C_8 coefficients for the interaction between the 16 combinations of alkali-metal atoms and the alkaline ions. Their breakdown contributions labeled as C_8^v, C_8^c, C_8^{VC}, and C_8^{CT} are obtained by using the corresponding polarizability contributions. We have given the references in square brackets and uncertainties in parentheses.

	Individual contributions to the C_8 coefficients					
	$C_8^v \times 10^{+5}$	C_8^c	$C_8^{VC} \times 10^{-4}$	$C_8^{CT} \times 10^{+4}$	Total (C_8)	Total (C_8) [52]
Li-Ca$^+$	0.68	6.86	0.0	−2.28	51749(9)	5.0478×10^4
Li-Sr$^+$	0.95	8.48	0.0	−2.59	69608(11)	6.7264×10^4
Li-Ba$^+$	1.59	30.21	0.0	−3.00	110737(28)	1.0540×10^5
Li-Ra$^+$	1.44	40.47	0.0	−2.53	103487(50)	
Na-Ca$^+$	0.78	44.31	0.0	−2.95	60720(10)	5.9725×10^4
Na-Sr$^+$	1.07	59.03	0.11	−3.37	80819(13)	7.8696×10^4
Na-Ba$^+$	1.75	177.76	0.56	−3.95	125566(28)	1.2032×10^5
Na-Ra$^+$	1.60	236.0	0.29	−3.35	118138(50)	
K-Ca$^+$	1.43	92.50	0.0	−6.78	116633(16)	1.1700×10^5
K-Sr$^+$	1.92	393.43	0.43	−7.76	153827(18)	1.5116×10^5
K-Ba$^+$	3.11	1044.87	2.35	−9.33	235841(31)	2.2784×10^5
K-Ra$^+$	2.77	1387.67	1.26	−7.94	218106(51)	
Rb-Ca$^+$	1.64	155.36	0.33	−8.17	139356(19)	1.3896×10^5
Rb-Sr$^+$	2.19	723.70	1.38	−9.36	183213(20)	1.7840×10^5
Rb-Ba$^+$	3.52	1823.03	5.23	−11.3	277748(32)	2.6626×10^5
Rb-Ra$^+$	3.12	2412.72	4.06	−9.60	256673(52)	

TABLE VIII. $E3$ matrix elements of Li, Na, K, and Rb atoms and Ca$^+$, Sr$^+$, Ba$^+$, and Ra$^+$ alkaline-earth ions calculated by using the DHF method.

Li		Na		K		Rb	
Contributions	$E3$ amplitude	Contributions	$E3$ amplitude	Contributions	$E3$ amplitude	Contributions	$E3$ amplitude
$2s_{1/2} \rightarrow 4f_{5/2}$	78.538	$3s_{1/2} \rightarrow 4f_{5/2}$	104.043	$4s_{1/2} \rightarrow 4f_{5/2}$	222.549	$5s_{1/2} \rightarrow 4f_{5/2}$	273.026
$2s_{1/2} \rightarrow 5f_{5/2}$	53.294	$3s_{1/2} \rightarrow 5f_{5/2}$	68.317	$4s_{1/2} \rightarrow 5f_{5/2}$	129.834	$5s_{1/2} \rightarrow 5f_{5/2}$	152.839
$2s_{1/2} \rightarrow 6f_{5/2}$	38.641	$3s_{1/2} \rightarrow 6f_{5/2}$	48.721	$4s_{1/2} \rightarrow 6f_{5/2}$	87.272	$5s_{1/2} \rightarrow 6f_{5/2}$	100.622
$2s_{1/2} \rightarrow 7f_{5/2}$	29.672	$3s_{1/2} \rightarrow 7f_{5/2}$	37.057	$4s_{1/2} \rightarrow 7f_{5/2}$	64.143	$5s_{1/2} \rightarrow 7f_{5/2}$	73.066
$2s_{1/2} \rightarrow 4f_{7/2}$	90.689	$3s_{1/2} \rightarrow 4f_{7/2}$	120.139	$4s_{1/2} \rightarrow 4f_{7/2}$	256.978	$5s_{1/2} \rightarrow 4f_{7/2}$	315.270
$2s_{1/2} \rightarrow 5f_{7/2}$	61.539	$3s_{1/2} \rightarrow 5f_{7/2}$	78.886	$4s_{1/2} \rightarrow 5f_{7/2}$	149.921	$5s_{1/2} \rightarrow 5f_{7/2}$	176.487
$2s_{1/2} \rightarrow 6f_{7/2}$	44.618	$3s_{1/2} \rightarrow 6f_{7/2}$	56.258	$4s_{1/2} \rightarrow 6f_{7/2}$	100.773	$5s_{1/2} \rightarrow 6f_{7/2}$	116.190
$2s_{1/2} \rightarrow 7f_{7/2}$	34.262	$3s_{1/2} \rightarrow 7f_{7/2}$	42.790	$4s_{1/2} \rightarrow 7f_{7/2}$	74.067	$5s_{1/2} \rightarrow 7f_{7/2}$	84.371
Ca$^+$		Sr$^+$		Ba$^+$		Ra$^+$	
Contributions	$E3$ amplitude	Contributions	$E3$ amplitude	Contributions	$E3$ amplitude	Contributions	$E3$ amplitude
$4s_{1/2} \rightarrow 4f_{5/2}$	90.926	$5s_{1/2} \rightarrow 4f_{5/2}$	119.888	$6s_{1/2} \rightarrow 4f_{5/2}$	168.517	$7s_{1/2} \rightarrow 5f_{5/2}$	165.834
$4s_{1/2} \rightarrow 5f_{5/2}$	36.939	$5s_{1/2} \rightarrow 5f_{5/2}$	41.240	$6s_{1/2} \rightarrow 5f_{5/2}$	29.028	$7s_{1/2} \rightarrow 6f_{5/2}$	19.939
$4s_{1/2} \rightarrow 6f_{5/2}$	20.554	$5s_{1/2} \rightarrow 6f_{5/2}$	20.712	$6s_{1/2} \rightarrow 6f_{5/2}$	2.200	$7s_{1/2} \rightarrow 7f_{5/2}$	5.845
$4s_{1/2} \rightarrow 7f_{5/2}$	13.485	$5s_{1/2} \rightarrow 7f_{5/2}$	12.668	$6s_{1/2} \rightarrow 7f_{5/2}$	4.941	$7s_{1/2} \rightarrow 8f_{5/2}$	10.916
$4s_{1/2} \rightarrow 4f_{7/2}$	104.994	$5s_{1/2} \rightarrow 4f_{7/2}$	138.446	$6s_{1/2} \rightarrow 4f_{7/2}$	194.625	$7s_{1/2} \rightarrow 5f_{7/2}$	191.567
$4s_{1/2} \rightarrow 5f_{7/2}$	42.654	$5s_{1/2} \rightarrow 5f_{7/2}$	47.607	$6s_{1/2} \rightarrow 5f_{7/2}$	33.443	$7s_{1/2} \rightarrow 6f_{7/2}$	22.487
$4s_{1/2} \rightarrow 6f_{7/2}$	23.734	$5s_{1/2} \rightarrow 6f_{7/2}$	23.902	$6s_{1/2} \rightarrow 6f_{7/2}$	2.575	$7s_{1/2} \rightarrow 7f_{7/2}$	6.848
$4s_{1/2} \rightarrow 7f_{7/2}$	15.570	$5s_{1/2} \rightarrow 7f_{7/2}$	14.614	$6s_{1/2} \rightarrow 7f_{7/2}$	5.601	$7s_{1/2} \rightarrow 8f_{7/2}$	12.476

evaluation of the dispersion coefficients. In practice, a number of methods have been employed for the calculations of the dispersion coefficients for the heteronuclear dimers. Dalgarno and Davison [55] have followed a procedure to reduce the two central molecular problems to one central atomic problem at larger separation distances. Bishop and Pipin [56] computed the C_6^{AB} coefficients by approximating the integral given by Eq. (14) using the Gaussian quadrature technique. In this work, we computed the dispersion coefficients by approximating the integral by the Gaussian quadrature of the integrand computed on the exponential grid of discrete imaginary frequencies. We justify the use of the exponential grid from the fact that maximum contributions to the integrand given in Eq. (14) arise from the polarizability values in the vicinity of zero frequency.

The coefficients C_6, C_8, and C_{10} of the R^{-6}, R^{-8}, and R^{-10} terms of the long-range atom-ion interactions are presented in Tables VI, VII, and IX, respectively. We present details of the calculated values of the C_6 dispersion coefficients for the interactions between the 16 combinations of alkali-metal atoms and the alkaline ions along with their breakdown

from the individual contributions such as valence (C_6^v), core (C_6^c), valence-core (C_6^{VC}), and cross terms (C_6^{CT}), respectively. From the tables, it can be inferred that the contribution to the total potential increases as the alkali-metal atoms get bigger in size (i.e., from the Li to Rb sequence), since the polarizability values also increase in the same order. The dominant contribution is from the valence part of the calculated results. We also observed that the core contribution to the C_6 and C_8 coefficients increases with the increasing number of electrons in the atom while the core-valence contribution to the total for some combinations is approximately zero. However, we notice that a steady increase in C_6 and C_8 values does not occur with respect to the atomic sizes for the ions (i.e., from Ca$^+$ to Ra$^+$). This might seem to be counterintuitive but it is owing to the fact that the polarizability of Ba$^+$ is larger than that for Ra$^+$, as given in Tables IV and V. So a different trend is followed with the dispersion coefficients: decreases in magnitude for the interactions of the alkali-metal atoms with Ra$^+$ and increases with Ba$^+$. Also we expect the accuracy of these coefficients to be on the same order as the dipole and

TABLE IX. Values of the C_{10} coefficients for interaction of the alkali-metal atoms with alkaline-earth ions. References are given in square brackets.

|	Total (C_{10})	Total (C_{10}) [52]		Total (C_{10})	Total (C_{10}) [52]
Li-Ca$^+$	4.0216×10^6	3.6586×10^6	K-Ca$^+$	1.5022×10^7	1.1358×10^7
Li-Sr$^+$	5.8214×10^6	5.0651×10^6	K-Sr$^+$	2.0433×10^7	1.5238×10^7
Li-Ba$^+$	9.2651×10^6	8.0669×10^6	K-Ba$^+$	3.0458×10^7	2.3604×10^7
Li-Ra$^+$	8.9619×10^6		K-Ra$^+$	2.8900×10^7	
Na-Ca$^+$	5.4726×10^6	4.6885×10^6	Rb-Ca$^+$	2.0147×10^7	1.4315×10^7
Na-Sr$^+$	7.7573×10^6	6.4345×10^6	Rb-Sr$^+$	2.7107×10^7	1.9101×10^7
Na-Ba$^+$	1.2056×10^7	1.0148×10^7	Rb-Ba$^+$	3.9986×10^7	2.9494×10^7
Na-Ra$^+$	1.1620×10^7		Rb-Ra$^+$	3.7746×10^7	
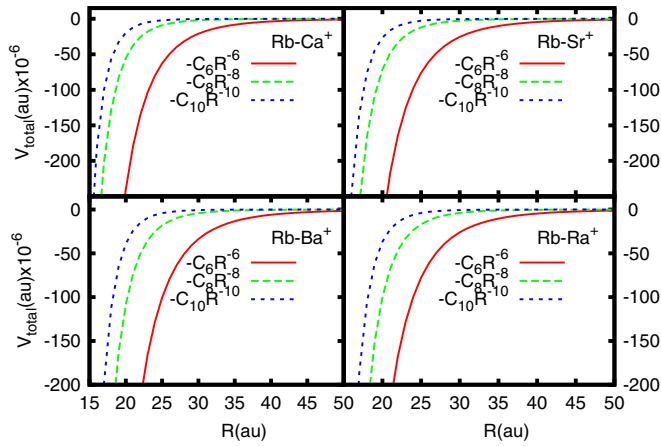
FIG. 1. (Color online) Dispersion coefficients C_6, C_8, and C_{10} (in a.u.) for different combinations of alkaline ions with the Rb atom as a function of internuclear distance (R) (in a.u.)

quadrupole polarizabilities of atoms and ions. The $E3$ matrix elements used to calculate the C_{10} coefficients estimated using the DHF method are given in Table VIII and numerical results for the coefficients are listed in Table IX. In Table IX we also compare our C_{10} coefficients with the recent theoretical calculations given by Jiang [52], who has used the oscillator strength sum rule. To our knowledge, no other results are available to compare the interaction of alkali-metal atoms with the Ra$^+$ ion.

From Tables VII and IX, it can be inferred that the magnitude of C_{10} and C_8 coefficients is more than that of C_6 coefficients for each atom-ion interaction. But their contribution to total interaction potential is much less because of the divisible factors of R^8 for C_8 and R^{10} for C_{10} as given in Eq. (13). Figure 1 highlights a comparison between the dispersion coefficients for the undertaken different combinations of the Rb atom with Ca$^+$, Sr$^+$, Ba$^+$, and Ra$^+$ ions, as a function of internuclear distance R. Interactions of

each alkaline ion (Ca$^+$, Sr$^+$, Ba$^+$, and Ra$^+$) are represented by the solid red line for the $C_6 R^{-6}$ coefficients, the long dashed green line for the $C_8 R^{-8}$ coefficients, and the short dashed blue line for the $C_{10} R^{-10}$ coefficients. It should be noted that our results for these potentials will be valid in the approximation only when the structures of the colliding atom and ion do not undergo internal changes.

V. CONCLUSION

In this work, we have deduced the behavior of the interaction potential for the alkali-metal atoms correlating with the alkaline-earth ions. The accurate values of the dipole and quadrupole polarizabilities for the alkali-metal atoms and the alkaline-earth ions have been investigated using the relativistic coupled-cluster method while the octupole polarizabilities are calculated using the DHF method. Evaluation of the dispersion coefficients has been done by integrating the product of atomic and ionic dynamic polarizabilities at imaginary frequencies. The calculated values of the induction coefficients in the form of a range of potentials are expected to be very useful to set the actual positions of the bound states and magnetic fields of the Feshbach resonances for these atom-ion correlated systems. Due to the lack of experimental data, we were unable to compare our theoretical values of the dispersion coefficients with the other measured values. The presented data will also be of immense interest for designing better atomic clocks, quantum information processing, and quantifying molecular potentials for ultracold collision studies.

[1] A. T. Grier, M. Cetina, F. Orucevic, and V. Vuletic, Phys. Rev. Lett **102**, 223201 (2009).

[2] Z. Idziaszek, T. Calarco, P. S. Julienne, and A. Simoni, Phys. Rev. A **79**, 010702(R) (2009).

[3] A. Härter and J. H. Denschlag, Contemporary Physics **55**, 33 (2014).

[4] J. Reichel and V. Vuletiĉ, *Atom Chips* (Wiley, Weinheim, Germany, 2011).

[5] M. Saffman, T. G. Walker, and K. Mølmer, Rev. Mod. Phys. **82**, 2313 (2010).

[6] C. Joachim, J. K. Gimzewski, and A. Aviram, Nature (London) **408**, 541 (2000).

[7] K. Ravi, S. Lee, A. Sharma, G. Werth, and S. Rangwala, Nature Communications **3**, 1126 (2012).

[8] F. H. J. Hall and S. Willitsch, Phys. Rev. Lett. **109**, 233202 (2012).

[9] D. J. Heinzen, R. Wynar, P. D. Drummond, and K. V. Kheruntsyan, Phys. Rev. Lett **84**, 5029 (2000).

[10] J. Goold, H. Doerk, Z. Idziaszek, T. Calarco, and T. Busch, Phys. Rev. A **81**, 041601 (2010).

[11] J. Joger, A. Negretti, and R. Gerritsma, Phys. Rev. A **89**, 063621 (2014).

[12] A. Rakshit and B. Deb, Phys. Rev. A **83**, 022703 (2011).

[13] L. Ratschbacher, C. Zipkes, C. Sias, and M. Köhl, Nat. Phys. **8**, 649 (2012).

[14] S. Willitsch, arXiv:1401.1699.

[15] R. Cote and A. Dalgarno, Phys. Rev. A **62**, 012709 (2000).

[16] H. N. Le, A. Kalev, M. D. Barrett, and B. G. Englert, Phys. Rev. A **85**, 052718 (2012).

[17] C. Sias and M. Köhl, arXiv:1401.3188.

[18] A. Derevianko, S. G. Porsev, and J. F. Babb, At. Data Nucl. Data Tables **96**, 323 (2010).

[19] S. Banerjee, J. A. Montgomery, J. N. Byrd, H. H. Michels, and R. Côté, Chem. Phys. Lett. **542**, 138 (2012).

[20] J. Mitroy and J. Y. Zhang, Eur. Phys. J. D **46**, 415 (2008).

[21] H. Doerk, Z. Idziaszek, and T. Calarco, Phys. Rev. A **81**, 012708 (2010).

[22] O. P. Makarov, R. Cote, H. Michels, and W. W. Smith, Phys. Rev. A **67**, 042705 (2003).

[23] L. W. Wansbeek, B. K. Sahoo, R. G. E. Timmermans, B. P. Das, and D. Mukherjee, Phys. Rev. A **78**, 012515 (2008).

[24] M. S. Safronova and U. I. Safronova, Phys. Rev. A **83**, 012503 (2011).

[25] D. Jiang, B. Arora, M. S. Safronova, and C. W. Clark, J. Phys. B **42**, 154020 (2009).

[26] W. Ansbacher, A. S. Inamdar, and E. H. Pinnington, Phys. Lett. A **110**, 383 (1985).

[27] A. Gallagher, Phys. Rev. **157**, 24 (1967).

[28] E. H. Pinnington, R. Berendst, and M. Lumsdent, J. Phys. B **28**, 2095 (1995).

[29] E. Iskrenova-Tchoukova and M. S. Safronova, Phys. Rev. A **78**, 012508 (2008).

[30] R. Pal, D. Jiang, M. S. Safronova, and U. I. Safronova, Phys. Rev. A **79**, 062505 (2009).

[31] Z. Idziaszek, A. Simoni, T. Calarco, and P. S. Julienne, New J. Phys. **13**, 083005 (2011).

[32] B. Arora, M. S. Safronova, and C. W. Clark, Phys. Rev. A **76**, 052509 (2007).

[33] B. K. Sahoo, Chem. Phy. Lett. **448**, 144 (2007).

[34] L.-Y. Tang, Z.-C. Yan, T.-Y. Shi, and J. Mitroy, Phys. Rev. A **81**, 042521 (2010).

[35] A. J. Thakkar and C. Lupinetti, Chem. Phys. Lett **402**, 270 (2005).

[36] U. I. Safronova, W. R. Johnson, and M. S. Safronova, Phys. Rev. A **76**, 042504 (2007).

[37] J. Mitroy and M. W. J. Bromley, Phys. Rev. A **68**, 052714 (2003).

[38] A. Miffre, M. Jacquey, M. Büchner, G. Trénec, and J. Vigué, Eur. Phys. J. D **38**, 353 (2006).

[39] C. R. Ekstrom, J. Schmiedmayer, M. S. Chapman, T. D. Hammond, and D. E. Pritchard, Phys. Rev. A **51**, 3883 (1995).

[40] W. F. Holmgren, M. C. Revelle, V. P. A. Lonij, and A. D. Cronin, Phys. Rev. A **81**, 053607 (2010).

[41] S. G. Porsev and A. Derevianko, J. Chem. Phys. **119**, 844 (2003).

[42] D. Spelsberg, T. Lorenz, and W. Meyer, J. Chem. Phys. **99**, 7845 (1993).

[43] M. Marinescu, H. R. Sadeghpour, and A. Dalgarno, Phys. Rev. A **49**, 982 (1994).

[44] B. K. Sahoo and B. Arora, Phys. Rev. A **87**, 023402 (2013).

[45] I. S. Lim and P. Schwerdtfeger, Phys. Rev. A **70**, 062501 (2004).

[46] E. S. Chang, J. Phys. B **16**, L539 (1983).

[47] P. S. Barklem and B. J. OMara, Mon. Not. R. Astron. Soc. **311**, 535 (2000).

[48] I. Miadokova, V. Kellö, and A. J. Sadlej, Theor. Chem. Acc. **96**, 166 (1997).

[49] E. L. Snow and S. R. Lundeen, Phys. Rev. A **76**, 052505 (2007).

[50] Y.-B. Tang, H.-X. Qiao, T.-Y. Shi, and J. Mitroy, Phys. Rev. A **87**, 042517 (2013).

[51] J. Mitroy, J. Y. Zhang, and M. W. J. Bromley, Phys. Rev. A **77**, 032512 (2008).

[52] J. Jiang, J. Mitroy, Y. Cheng, and M. W. J. Bromley, Atomic Data and Nuclear Data Tables **101**, 158 (2015).

[53] B. Arora, D. K. Nandy, and B. K. Sahoo, Phys. Rev. A **85**, 012506 (2012).

[54] B. K. Sahoo, and B. P. Das, Phys. Rev. A **86**, 022506 (2012).

[55] A. Dalgarno and W. D. Davison, Adv. At. Mol. Phys. **2**, 1 (1966).

[56] D. M. Bishop and J. Pipin, J. Chem. Phys. **97**, 3375 (1992).